Marine Chemistry 111 (2008) 199–213

Contents lists available at ScienceDirect

Marine Chemistry

journal homepage: www.elsevier.com/locate/marchem

Sources of molecularly uncharacterized organic carbon in sinking particles from three ocean basins: A coupled $\Delta^{14}C$ and $\delta^{13}C$ approach

Leslie A. Roland [a], Matthew D. McCarthy [a,*], Tom Guilderson [a,b]

[a] Department of Ocean Sciences, University of California, 1156 High Street, Santa Cruz, CA 95064, United States
[b] Center for Accelerator Mass Spectrometry, Lawrence Livermore National Laboratory, 7000 East Avenue, Livermore, CA 94550, United States

ARTICLE INFO

Article history:
Received 20 April 2007
Received in revised form 9 May 2008
Accepted 13 May 2008
Available online 19 July 2008

Keywords:
Carbon isotopes
Particulate organic matter
Organic constituents
Resuspended sediments
Non-selective preservation
Composition

ABSTRACT

Several recent studies have suggested dramatically different ideas about the source and nature of molecularly uncharacterized organic carbon (MUC) in sinking marine particles (POC). Carbon isotope data coupled with hydrolysis has indicated MUC is lipid-like material, suggesting selective preservation [Hwang, J. and Druffel, E.R.M., 2003. Lipid-like material as the source of the uncharacterized organic carbon in the ocean? Science, 299: 881–884.]. In contrast, NMR-based work has strongly indicated non-selective degradation, with amino acid dominating resistant material [Hedges, J.I. et al., 2001. Evidence for non-selective preservation of organic matter in sinking marine particles. Nature, 409: 801–804.]. This study set out to explore this seeming paradox, and to examine the hypothesis that the nature of MUC may vary strongly between margin and open ocean regions. We examined the coupled elemental, stable and radiocarbon isotopic compositions of three fractions of sinking POC: lipids, acid soluble (AS) material (a proxy for hydrolyzable biomolecules), and acid insoluble (AI) material (a proxy for the MUC). $\Delta^{14}C$ and $\delta^{13}C$ measurements were made on three time-series of sediment trap samples in widely separate ocean regions: Santa Barbara Basin, Cariaco Basin, and an oceanic site in the Eastern Subtropical Atlantic off Dakar, Africa.

$\Delta^{14}C$ compositions of AI fractions at all sites indicated substantial contribution by pre-aged marine carbon sources (40–60% of total sinking POC), not derived from direct export of surface productivity. Comparison of $\delta^{13}C$ and $\Delta^{14}C$ values with coexisting lipid and AS signatures also suggested widely different AI compositions from different ocean environments. AI material in coastal California waters consistently appeared lipid-like, in agreement with several studies near the same region [Hwang, J. and Druffel, E.R.M., 2003. Lipid-like material as the source of the uncharacterized organic carbon in the ocean? Science, 299: 881–884.; Hwang, J., Druffel, E. R.M., Eglinton, T.I. and Repeta, D.J., 2006b. Source(s) and cycling of the nonhydrolyzable organic fraction of oceanic particles. Geochimica et Cosmochimica Acta, 70: 5162–5168.]. In contrast, our oceanic site's AI isotopic signatures were more consistent with non-selective preservation of a range of biochemical classes. AI compositions in Cariaco Basin proved to be variable with time, suggesting a complex and variable mixture of AI sources.

These results suggest a major divergence between coastal and oceanic AI sources and composition. Taken together, we propose that the dominant mechanism influencing molecularly uncharacterized material is non-selective preservation during initial water column transit; influenced to varying degrees by subsequent addition of allochthonous and ^{14}C-depleted organic carbon sources. In our coastal margin sites, all AI properties point to resuspended sediment as the most likely source of total uncharacterizable POC. In our more oceanic site, where particles have much longer transit times, incorporation of old DOC into POC, in addition to resuspended sediment, may have a substantial influence on overall $\Delta^{14}C$ ages. We propose that major differences between AI compositions in different locations is tied to

* Corresponding author. Tel.: +1 831 459 4718.
E-mail address: mccarthy@pmc.ucsc.edu (M.D. McCarthy).

0304-4203/$ – see front matter
doi:10.1016/j.marchem.2008.05.010

variation in availability of such pre-aged OC sources, linked to regional oceanographic conditions and strongly influenced by proximity to continental shelves. The strong correlations we observe between %AI vs. %AS composition and elemental and isotopic values also implies that substantial amounts of POC collected via sediment traps in some locations is not exported directly from surface production, but added from other pre-aged reservoirs.

1. Introduction

Sinking particulate organic carbon (POC) is a major reservoir of reduced carbon in the ocean. The flux of POC to the ocean's interior is the "biological pump", which acts to maintain the ocean's balance of bioactive elements and nutrients, supports microbial and benthic communities, and preserves a long-term geochemical record of ocean history in accumulating sediments. While greater than 90% of sinking POC is remineralized in the upper ocean (e.g., Suess, 1980), remaining particles appear to undergo a significant transformation during transit through the water column. At the surface, more than 80% of POC can be characterized as major biochemicals (amino acids, carbohydrates, lipids and pigments; e.g., Wakeham et al., 1997b), but with increasing depth the characterizable fraction falls dramatically. Below the mesopelagic zone less than 30% of POC can be compositionally characterized using current methods, while at the sediment–water interface typically less than 20% can be identified (Wakeham et al., 1997b). The mechanisms regulating this change (and controlling the linkage between upper ocean productivity and sedimentary carbon preservation) are not well understood, however, they have profound implications for the ocean carbon cycle.

There are a number of hypotheses for the origin of uncharacterizable organic material in sinking particulate organic matter (POM) (e.g., Lee et al., 2005). Some of these include geomacromolecule formation (deLeeuw and Largeau, 1993; Tegelaar et al., 1989), organic-inorganic associations (Armstrong et al., 2002; Hedges and Keil, 1995), encapsulation or organic associations (Hill, 1998; Nagata and Kirchman, 1997), and selective degradation/preservation (Hwang and Druffel, 2003; Largeau and deLeeuw, 1995; Minor et al., 2003). Recent studies have employed several novel techniques to understand the composition of uncharacterized POM, but have in some cases reached dramatically different conclusions. Hedges et al. (2001) applied solid-state ^{13}C-Nuclear Magnetic Resonance (NMR) to examine relative spectral signatures of total sinking POM through the water column in the equatorial Pacific and Arabian Sea. By comparing spectra from surface vs. deep sediment-trap samples, these authors concluded that the uncharacterized component is mainly composed of amino acid-like material, with major compound class ratios unchanged from surface POM. Because amino acids are among the most labile and readily remineralized biochemicals, they suggested non-selective preservation, perhaps facilitated by an inorganic matrix providing physical protection from degradation (Lee et al., 2000). In contrast, Hwang and co-authors (Hwang and Druffel, 2003; Hwang et al., 2006a,b) analyzed samples from Station M in the California (CA) Current, using combined radiocarbon (Δ^{14}C) and stable carbon (δ^{13}C) isotopic signatures of major biochemical classes compared with those found in uncharacterized acid-insoluble material. These data indicated that lipid-like compounds dominated the uncharacterizable fraction, thus strongly suggesting a selective preservation mechanism (Hwang and Druffel, 2003). Together these contrasting studies seem to suggest not only extremely different molecular compositions for molecularly uncharacterized POM, but also essentially opposed mechanisms of preservation.

In this work we have examined one potential explanation for these contrasting results: that unidentified material in coastal vs. oceanic POM may have fundamentally different sources and compositions. While none of the common mechanisms of organic carbon preservation are mutually exclusive, it is possible that the dominant preservation process could vary in different oceanic regimes. For example, if selective preservation were dominant, variations in plankton sources and communities might lead to the greater preservation of certain compound groups in specific ocean regions or productivity conditions. In contrast, abiotic formation of complex geopolymers from common biomolecule precursors might be predicted to be a more universal process (deLeeuw and Largeau, 1993; Fandino et al., 2001; Pinhassi et al., 2003). One key to differentiating between different mechanisms may lie in applying new analytical approaches to probe unidentifiable material having contrasted sources or composition.

We applied coupled δ^{13}C and Δ^{14}C analysis to isolated POC fractions and the acid-insoluble (uncharacterized) fraction in three distinct oceanic regimes: the Northwest Atlantic margin, the CA margin and oceanic Atlantic Ocean. Following the approach of Hwang and Druffel (2003), we compared isotopic signatures of the isolated fractions with remaining non-hydrolyzable material in order to assess its relative sources. We also expanded this approach by examining material resistant to different forms of acid hydrolyses. Our results suggest that the apparently contradictory results discussed above may in fact be explained by differences in the dominant hydrolysis-resistant material in oceanic vs. margin environments, which can be linked to varying sources of allochthonous (pre-aged, non-surface derived) organic material in different oceanographic regimes.

2. Methods

2.1. Study sites and sampling methods

Samples were collected in sediment traps from three distinct ocean regions: two highly productive continental margin sites in the NE Pacific and NW Atlantic Oceans, and one open ocean site in the Eastern Subtropical Atlantic. POC samples were obtained in conjunction with several long-term monitoring efforts. Santa Barbara Basin (SBB) and Cariaco Basin (CAR) samples were collected by the Marine Sediments Research Lab at University of South Carolina as part of ongoing projects in those basins. Eastern Subtropical Atlantic (ESA) samples were generously provided by Dr. Leslie Sautter of the College of Charleston.

The NE Pacific site is located in the Santa Barbara Basin (34°14′N, 120°02′W; Fig. 1), 20 km offshore of central CA. Trap samples were collected at a water depth of 450 m from October 1999–March 2000, 150 m above the basin depth. The surface waters in this region lie in the California Current system, are highly productive due to strong spring and early summer upwelling (Lange et al., 1997), and also have episodic terrestrial input from runoff and precipitation occurring in the fall and winter months (Thunell et al., 1995).

The second margin site located in the NW Atlantic Ocean is the Cariaco Basin (10°30′N, 64°40′W; Fig. 1) located 30 km off the northern coast of Venezuela. CAR samples were collected as a part of the CARIACO (CArbon Rentention In A Colored Ocean) time series, a multinational, multidisciplinary mooring project. The deepest part of the basin is 1400 m, therefore sinking POC samples were collected at depths of 275 m, 930 m and 1255 m from November 1998–October 1999. Depths below ~300 m exist in anoxic conditions due to poor and infrequent ventilation and degradation of organic matter (Astor et al., 2003; Deuser, 1973). CAR also experiences upwelling-driven periods of high productivity linked to the seasonal migration of the inter-tropical convergence zone (ITCZ). The Tuy, Unare, Neveri, and Manzanares rivers drain a minor fraction of terrestrial organic matter directly into the basin (Peterson and Haug, 2006). Since the water column is anoxic below 300 m, sinking particles are well preserved at depth and in the underlying sediments, where decomposition rates diminish with older compounds (Hulthe et al., 1998).

The ESA open ocean site is located in the Eastern Subtropical Atlantic (15°5'N, 19°5'W; Fig. 1), 220 km northwest off the coast of Africa. A single sediment trap was moored at 3317 m, 300 m above the seafloor, from June 1993 to June 1994. At this site, trade winds and the migrating ITCZ also result in significant seasonality in surface production (Wefer and Fisher, 1993). Unlike the other sites, this regime has a fully oxic water column and productivity is likely more influenced by picoplankton and microbial loop processes than either coastal site.

At all sites, automated Mark VII cone-shaped sediment traps (Honjo and Doherty, 1988) were used for POM collection, with 13-automated cups collecting subsamples at 2-week intervals in each cup. CAR samples were poisoned with 3% formaldehyde, whereas SBB and ESA samples were treated with sodium azide. Formalin preservation can potentially enrich carbon relative to nitrogen; whereas sodium azide can result in nitrogen enrichment (by ~1‰). In practice, however, both treatments have been shown to have minimal impacts on observed C/N_{at} ratios, %TOC, total nitrogen (%TN), $\Delta^{14}C$, and $\delta^{13}C$ isotopes (Altabet, 2001; Honda, 1996; Nakatsuka et al., 1998; Hedges et al., 1993; Knauer et al., 1984). Specifically, Honda et al. measured $\Delta^{14}C$ in sinking POC preserved in 5% formalin and found no significant change over varying storage times from months to years. The same relationship can be inferred for specific compound classes (e.g., amino acids) since they largely contribute to bulk POC. Samples were rinsed several times with distilled water and if "swimmers" were present, they were quickly removed. Samples were stored refrigerated until analysis (Woodworth et al., 2004). Before analysis samples were centrifuged, frozen, lyophilized and ground to fine particulates. As indicated above, samples from CAR were collected from a sediment trap at the oxycline (275 m) and two deeper sediment traps on the same mooring (930 m and 1255 m). Limited POC material from deeper traps necessitated using samples with enough material from either 930 m or 1255 m traps at different time periods to constitute a deep sample for analysis. In what follows we thus refer to only "shallow" (275 m) and "deep" (930 m or 1255 m) samples. For the ESA samples, it was necessary to combine several two-week collections in order to provide enough material for analysis.

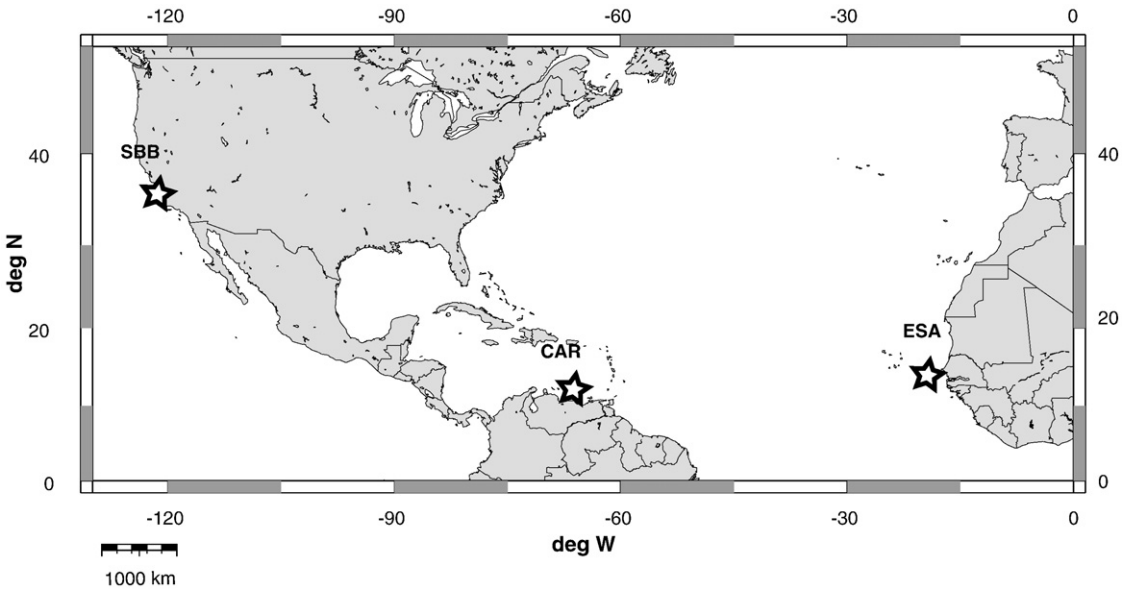

Fig. 1. Sampling locations. Stars indicate Pacific and Atlantic margin sediment trap sites (SBB and CAR), and Atlantic oceanic site (ESA). Abbreviations are as defined in text; sample locations are as described in methods.

2.2. POC fraction extractions and isolations

POC fractions were isolated using methods described previously in detail (Hwang and Druffel, 2003; Hwang et al., 2006b; Wang et al., 1998). Briefly, subsamples (~20 mg) for bulk analysis were separated and directly acidified overnight with 1N HCl to remove inorganic carbon, then dried at 50 °C. Lipids were extracted from the POM (100–300 mg for CAR, 200–500 mg for SBB, 800–1000 mg for ESA; vs. 1000 mg in previous coastal studies) using a 2:1 (v:v) dichloromethane/methanol mixture. Samples were vortexed, sonicated and centrifuged five times, or until supernatant was colorless. The combined extract was dried in a stream of N_2, acidified with 1 N HCl to remove any residual inorganic carbon, and transferred to precombusted quartz tubes. The lipid-extracted POC was oven-dried and split into two fractions for acid hydrolyses.

Independent acid hydrolyses were used to isolate two acid insoluble (AI) fractions. The acid insoluble-amino acid (AI–AA) fraction consisted of material resistant to HCl hydrolysis, under conditions commonly used for amino acid analysis (6 N HCl at 100 °C for 19 h; e.g., Lee and Cronin, 1982); the insoluble organic matter remaining after this treatment was defined as the AI–AA fraction. The acid insoluble-carbohydrate (AI-CHO) similarly consisted of material resistant to H_2SO_4 hydrolysis, under conditions commonly used to analyze carbohydrates from marine organic matter (72% H_2SO_4 at room temperature for 2 h, dilution to 1.2N H_2SO_4 and hydrolysis at 100°C for 3 h; e.g., Cowie and Hedges, 1984). The H_2SO_4-resistant organic matter remaining in solid phase after this treatment was isolated by centrifugation, and defined as AI-CHO. Amino acid and carbohydrate isotope analysis were attempted, but small sample sizes relative to the blanks associated with the column (ion exchange resin) purification methods (Hwang and Druffel, 2005) precluded the direct isolation and isotopic measurement of amino acid or carbohydrate fractions.

2.3. Isotope measurements

Total POC samples, lipid extracts and independently obtained AI fractions were transferred to precombusted (4 h at 900 °C) quartz tubes for $\Delta^{14}C$ and $\delta^{13}C$ measurements. Briefly, pre-combusted CuO pellets were added in addition to Ag powder, then tubes were evacuated to $<10^{-3}$ Torr and flame-sealed under vacuum. Sealed tubes were combusted for 3.5 h at 900 °C. The resulting CO_2 was cryogenically purified, measured, and then reduced to elemental carbon in the presence of an iron catalyst and a stoichiometric excess of hydrogen gas (e.g., Vogel et al., 1987, 1984). If enough CO_2 was present (>300 μg C), subsamples for ^{13}C were recovered. CO_2 for $\Delta^{14}C$ was graphitized and pounded into targets for accelerator mass spectrometry (AMS) analysis. Radiocarbon analyses were made at the Center for Accelerator Mass Spectrometry (CAMS) at Lawrence Livermore National Labs (UC/LLNL). The $\delta^{13}C$, small sample, and background corrected fraction modern values were further used to reduce and report an absolute $\Delta^{14}C$ equivalent to "age-corrected" $\Delta^{14}C$ for known-age materials, where we use the mid-point of the sediment trap deployment for the known year (Stuiver and Polach, 1977). This allows us to report the $\Delta^{14}C$ for the material in the year that it was trapped and removed from the ocean. The modern and dead carbon contributed during sample graphitization for small samples is corrected as described by Brown and Southon (Brown and Southon, 1997). Off-line $\delta^{13}C$ measurements of CO_2 splits were preformed at the UC Davis Stable Isotope Facility following standard protocols. Bulk POC and AI fraction $\delta^{13}C$ measurements were made at either UC Santa Cruz or UC Davis light stable isotope facilities using continuous flow elemental analyzer–isotope ratio mass spectrometer (EA-IRMS) systems.

2.4. Mass balance calculations and regression analysis

Isotope values for the acid-soluble (AS) fraction were calculated by direct mass-balance (Eqs. (1) and (2)):

$$\Delta^{14}C_{AS} = \left[\left(\Delta^{14}C_{Bulk}\right) - \left(f_{AI(avg)} \times \Delta^{14}C_{AI(avg)}\right) - \left(f_{Lipid} \times \Delta^{14}C_{Lipid}\right)\right] / f_{AS} \quad (1)$$

$$\delta^{13}C_{AS} = \left[\left(\delta^{13}C_{Bulk}\right) - \left(f_{AI(avg)} \times \delta^{13}C_{AI(avg)}\right) - \left(f_{Lipid} \times \delta^{13}C_{Lipid}\right)\right] / f_{AS} \quad (2)$$

where $f_{AS} = 1 - f_{AI(avg)} - f_{Lipid}$.

$AI_{(avg)}$ represents *average* values of combined AI-AA and AI-CHO for each sample, whereas f is the fraction of each

Table 1
Percent carbon recoveries for sample fractions

Sample	% Carbon recovery					
	AI-AA	AI-CHO	AI-avg	AA/CHO	LE	AS[a]
CAR 7A #3	47	42	44	1.1	7	49
CAR 7A # 7	13	34	24	0.4	15	61
CAR 8A #2	26	29	28	0.9	4	68
CAR 8A #4	33	18	25	1.9	5	70
CAR 8A # 10	60	47	53	1.3	8	39
CAR 8A #12	66	39	52	1.7	11	37
Average	41	35	38	1.2	8	54
S.D.	20	10	14	0.5	4	14
CAR 7D #3	38	44	41	0.9	6	53
CAR 7D #7	34	28	31	1.2	24	45
CAR 8C #2	36	51	43	0.7	5	52
CAR 8C #4	41	46	43	0.9	10	47
CAR 8C #10	37	47	42	0.8	11	47
CAR 8C #12	24	66	45	0.4	9	46
Average	35	47	41	0.8	11	49
S.D.	6	12	5	0.3	7	3
SBB 12 #3	52	57	55	0.9	6	39
SBB 12 #5	61	62	61	1.0	5	34
SBB 12 #9	64	70	67	0.9	4	28
SBB 12 #13	67	72	70	0.9	6	25
SBB 13 #2	62	69	66	0.9	4	30
SBB 13 #4	72	76	74	0.9	5	21
Average	63	68	65	0.9	5	30
S.D.	7	7	7	0.0	1	6
ESA #1	50	73	61	0.7	4	35
ESA #2	46	73	60	0.6	3	37
ESA #3	25	76	50	0.3	3	47
Average	40	74	57	0.5	3	40
S.D.	14	2	6	0.2	1	6

Fraction abbreviations as defined in text; LE = lipid extraction; AA/CHO = the ratio of AI-AA vs AI-CHO recoveries. Averages and standard deviations (S.D.) also shown for samples within each site and sample group.

[a] AS percent calculated by subtracting AI-avg and LE fractions.

Table 2
Samples, collection periods, bulk isotopic and elemental composition

Date	Sample	Depth (m)	%N	%OC	C/N_{at}	CAMS #	$\Delta^{14}C$ (‰)	$\delta^{13}C$ (‰)
Dec-98	CAR 7A #3	275	0.8	5.5	7.7	117957	21±4	−21.8
Feb-99	CAR 7A # 7	275	2.2	14.5	7.5	117958	48±4	−19.2
May-99	CAR 8A #2	275	1.7	10.1	7.0	113739	40±7	−21.0
Jun-99	CAR 8A #4	275	1.5	9.6	7.3	125373	49±11[a]	−21.6
Sep-99	CAR 8A # 10	275	0.7	5.1	8.1	113740	−7±5	−21.8
Oct-99	CAR 8A #12	275	0.6	4.4	8.3	125374	−4±3[a]	−21.5
Dec-98	CAR 7D #3	1255	1.0	6.8	7.6	121374	56±4	−21.8
Feb-99	CAR 7D #7	1255	1.9	14.0	8.4	121375	29±4	−19.0
May-99	CAR 8C #2	930	0.7	5.4	8.6	121376	23±4[a]	−22.1
Jun-99	CAR 8C #4	930	1.3	8.9	8.1	121377	46±2[a]	−22.0
Sep-99	CAR 8C #10	930	0.9	5.8	7.4	121378	32±4	−22.1
Oct-99	CAR 8C #12	930	0.5	3.3	7.7	121379	9±4	−22.2
May-99	SBB 12 #3	450	0.6	4.4	8.2	117961	−52±5	−21.3
Jun-99	SBB 12 #5	450	0.5	3.7	8.5	125378	−57±13[a]	−21.8
Aug-99	SBB 12 #9	450	0.5	3.6	8.6	117964	−67±3	−21.6
Oct-99	SBB 12 #13	450	0.4	3.4	9.0	113742	−97±4	−22.1
Nov-99	SBB 13 #2	450	0.5	3.8	8.8	125377	−68±2[a]	−21.3
Dec-99	SBB 13 #4	450	0.4	3.3	8.9	117962	−94±3	−21.7
Jun-93	ESA #1	3317	0.2	1.7	9.5	125370	25±5	−21.0
Sep-93	ESA #2	3317	0.2	1.4	10.1	125371	23±4	−21.3
Mar-94	ESA #3	3317	0.2	1.3	9.1	125372	40±4	−20.2

Abbreviations as defined in text. CAR (A) represents upper water traps in Cariaco Basin, CAR (C, D) are the combined samples for deep water traps. CAMS # indicates LLNL accelerator faculty internal tracking identification. Average $\delta^{13}C$ error ± 0.2‰. $\Delta^{14}C$ error values denoted by (a) are deviations from duplicate analysis, while all other errors come from the AMS instrument.

compound class. Associated ^{14}C AS errors were by propagated from AI and lipid errors, which likely does not represent real, environmental error. However, AI and AS regression analyses across all sample sites indicated that whatever error may exist in an individual sample does not affect the resulting discussion or conclusions. The AS fraction in suspended POC has recently been shown to primarily constitute combined hydrolyzable amino acid and carbohydrate compound classes, but also includes a small component of additional macromolecules (Hwang and Druffel, 2006). Reduced Major Axis (RMA) regression statistical analysis was done in RMA software v.1.20: Java Version (Bohonak and van der Linde, 2004) to calculate R^2 and y-intercepts values. RMA is a statistical program that accounts for errors in both x- and y-variables and compiles R^2 and y-intercepts from the average of 1000 bootstrap runs. p-values were calculated in SYSTAT 12 by linear regression analysis. The lower the p-value, the increased significance of a correlation. For $p<0.05$, correlations are judged to be highly significant ($\alpha=0.05$).

3. Results

Carbon recoveries for each isolated fraction are given in Table 1. Bulk isotopic, TOC, TN and C/N_{at} results for all sites are summarized in Table 2. Data for lipids, independently isolated AI fractions, and AS material are reported in Table 3. Regression results for relative AS and AI content vs. isotopic values and elemental ratios are found in Table 4, including R^2, p-values and y-intercepts for projected "pure" AS and AI material.

3.1. Carbon recoveries

All traps had relatively large fractions of TOC present as AI material, consistent with previous studies of subsurface and deep sinking POC (Hwang and Druffel, 2003; Wakeham et al., 1997b; Wang et al., 1998). Recoveries of AI from the two isolation approaches were very close in the two margin sites, however they

Table 3
Stable and radiocarbon values for AI, lipid extracts, and calculated AS fractions

Sample	Depth (m)	AI-AA (‰)			AI-CHO (‰)			Lipid (‰)			AS* (‰)	
		CAMS #	$\Delta^{14}C$	$\delta^{13}C$	CAMS #	$\Delta^{14}C$	$\delta^{13}C$	CAMS #	$\Delta^{14}C$	$\delta^{13}C$	$\Delta^{14}C$	$\delta^{13}C$
CAR 7A #3	275	118002	−56±4	−23.5	118009	−33±3	−22.6	121365	−15±3	−25.1	85±3	−20.2
CAR 7A # 7	275	127884	−22±10	−21.0	118010	36±4	−20.5	121366	36±3	−21.8	67±6	−17.9
CAR 8A #2	275	113743	−20±4	−24.0	113747	−13±4	−23.2	121373	58±4	−25.6	62±4	−19.6
CAR 8A #4	275	125509	−34±8[a]	−23.8	118011	−38±21[a]	−22.4	125499	19±14[a]	−24.4	81±14	−20.8
CAR 8A # 10	275	113744	−61±5	−20.7	113748	−26±4	−23.3	121636	9±3	−24.7	39±4	−20.9
CAR 8A #12	275	125381	−78±6[a]	−23.0	125513	−60±1[a]	−22.3	125500	−50±2[a]	−25.1	100±3	−18.9
CAR 7D #3	1255	121386	−21±3	−23.3	121392	−17±4	−22.7	121380	34±3	−24.9	116±3	−20.6
CAR 7D #7	1255	121387	4±3	−21.0	121393	37±3	−20.1	–	n.d.	n.d.	n.d.	n.d.
CAR 8C #2	930	121388	−23±10[a]	−23.4	121394	−20±5[a]	−22.8	125501	23±17[a]	−25.2	64±11	−20.9
CAR 8C #4	930	121389	−6±7a	−23.0	125515	2±5a	−22.6	125502	48±7[a]	−24.6	90±6	−20.7
CAR 8C #10	930	121390	−50±4	−23.8	121646	−25±3	−22.5	121383	40±4	−25.8	92±4	−20.2
CAR 8C #12	930	121391	−65±3	−23.6	121647	−37±3	−22.7	121384	39±3	−25.4	61±3	−20.7
SBB 12 #3	450	118005	−94±4	−22.7	121654	−128±3	−23.0	121369	−66±4	−23.7	32±4	−18.9
SBB 12 #5	450	125510	−121±3[a]	−23.2	118014	−145±17[a]	−22.8	125504	−108±6[a]	−24.1	87±9	−19.3
SBB 12 #9	450	118008	−76±5	−22.6	118015	−202±3	−23.1	121371	−117±3	−23.4	111±4	−18.4
SBB 12 #13	450	113746	−188±5	−24.2	127885	−152±3	−23.5	113753	−379±2	n.d.	174±3	n.d.
SBB 13 #2	450	113745	−139±27[a]	−23.9	113749	−131±7[a]	−23.3	125503	−135±6[a]	−23.4	89±13	−15.8
SBB 13 #4	450	118006	−147±5	−22.8	118013	−204±5	−23.5	118017	−217±3	n.d.	218±4	n.d.
ESA #1	3317	125506	−1±4	−22.0	127886	−4±3	−21.9	125379	−55±4	−23.9	82±4	−18.9
ESA #2	3317	125507	−2±2	−22.1	125511	−11±5	−21.8	125380	−91±3	−24.2	78±3	−20.0
ESA #3	3317	125508	16±3	−21.3	125512	13±6	−21.4	125498	−55±4	−24.0	73±4	−18.6

Abbreviations as defined previously. n.d. = no data. Average $\delta^{13}C$ error ± 0.2‰. $\Delta^{14}C$ error values denoted by (a) are deviations from duplicate analysis, while all other errors come from the AMS instrument. *AS values are calculated by mass balance equations using AI-avg and lipid values, as explained in text (refer to Section 2.4). However, associated ^{14}C AS errors were propagated from AI and lipid errors, which likely does not represent real, environmental error.

Table 4
Results of reduced major axis regression analyses

Location	Radiocarbon ($\Delta^{14}C$)				Elemental ratio (C/N_{at})				Stable carbon ($\delta^{13}C$)			
	x=%(AI+lipid) y-int=AS		x=%(AS+lipid) y-int=AI		x=%(AI+lipid) y-int=AS		x=%(AS+lipid) y-int=AI		x=%(AI+lipid) y-int=AS		x=%(AS+lipid) y-int=AI	
	R^2, p	y-int	R^2, p	y-int	R^2, p	y-int	R^2, p	y-int	R^2, p	y-int	R^2, p	y-int
CAR-sfc	**0.92, 0.00**	**+105**	**0.97, 0.00**	**−92**	**0.92, 0.00**	**6.1**	**0.78, 0.02**	**9.9**	0.15, 0.45	−18.0	0.37, 0.19	−25.7
CAR-deep	0.20, 0.38	+291	0.02, 0.83	−165	0.00, 0.96	15	0.14, 0.46	2.3	0.18, 0.42	−40.9	**0.96, 0.00**	**−36.3**
SBB	**0.83, 0.01**	**+135**	**0.81, 0.02**	**−169**	**0.81, 0.01**	**5.4**	**0.85, 0.01**	**10.2**	0.28, 0.30	−18.3	0.25, 0.33	−23.2
ESA	0.93, 0.20	+117	0.96, 0.12	−36	0.49, 0.55	4.8	0.56, 0.47	13.1	0.83, 0.32	−15.5	0.88, 0.24	−24.9

For each sample group, reduced major axis regression results for $\Delta^{14}C$, C/N_{at} and $\delta^{13}C$ in bulk POC vs. two versions of percentage AI or AS composition are shown. The two regression versions differ by assignment of the lipid fraction. For x=%(AI+lipid), the resulting y-intercept predicts 'pure AS'. For x=%(AS+lipid), the resulting y-intercept predicts 'pure AI'. For each regression R^2, p-value (significant likelihood for $p<0.05$) and y-intercept are reported. Bold text indicates significant correlation (high R^2 and $p<0.05$).

differed in the more open ocean ESA site (Table 1). In CAR traps, average AI recovery was 39% of TOC from both treatments (AI-AA=38%, AI-CHO=41%); while at SBB, average AI was 65% of TOC (AI-AA=63%, AI-CHO=68%). In ESA samples, overall AI recoveries were higher (averaging 57%), however recoveries from the two hydrolysis treatments diverged (AI-AA=40%, AI-CHO=74%). These recovery values were used along with isotope values to calculate AS isotopic values as described above. Extractable lipids were 3–11% of total carbon in all samples (averages: CAR=9%; SBB=5%; ESA=3%). The extractable lipid recoveries and resulting AS estimates are similar to those that have been previously reported (Hwang and Druffel, 2003; Wang et al., 1998) for sinking POC using similar analytical approaches.

3.2. Santa Barbara Basin (SBB)

Bulk POC stable isotopic values were consistent with marine origin, with $\delta^{13}C$ values ranging from −21.3‰ to −22.1‰ (Table 2; Fig. 2a). The C/N_{at} ratios ranged from 8.2 to 8.9. Bulk POC $\Delta^{14}C$ values ranged from −52‰ to −97‰, with highest values observed in May (Table 2; Fig. 2b). These $\Delta^{14}C$ values are substantially lower than those from POC at the other sites in this study. Percentages of TOC (3.3% to 4.4%) and TN (0.4% to 0.6%) were also similar throughout the time-series, with somewhat higher OC values in the summertime and lower values in the winter months.

AI fractions had generally depleted isotopic values than those found in bulk sinking particles. AI-AA $\delta^{13}C$ ranged from −22.6‰ to −24.2‰, while AI-CHO ranged from −22.8‰ to −23.5‰ (Table 3; Fig. 2a). Radiocarbon values of AI were also depleted relative to bulk POC. $\Delta^{14}C$ for AI-AA ranged from −76‰ to −188‰, and AI-CHO from −128‰ to −204‰ (Table 3; Fig. 2b). Overall, AI-AA and AI-CHO fractions at SBB had very similar isotopic values, falling within ±0.4‰ for $\delta^{13}C$ and ±29‰ for $\Delta^{14}C$. The extractable lipid fractions generally resembled AI values in both $\delta^{13}C$ and $\Delta^{14}C$ for most samples. Lipid stable carbon values ranged from −23.4‰ to −24.1‰, with $\Delta^{14}C$ ranging from −66‰ to −379‰. Calculated AS $\delta^{13}C$ and $\Delta^{14}C$ values ranged from −15.8‰ to −19.3‰ and 32‰ to 218‰, respectively.

Regression analyses were conducted for percentage composition of AS and AI vs. $\delta^{13}C$, $\Delta^{14}C$, and C/N_{at}. Two regressions versions were run, the first with x=%(AI+Lipid), such that the y-interercept=predicted "pure" AS; and the second with x=%(AS+Lipid), such that the y-intercept is predicted "pure" AI. AS vs. ^{14}C correlations had R^2 and p-values of 0.83 and 0.01, while AI vs. ^{14}C had R^2 and p-values of 0.81 and 0.02 (Table 4). The y-intercepts for pure AS and pure AI predicted ^{14}C values of 135‰ and −169‰, respectively. C/N_{at} regressions had similar R^2 and p-values of 0.81 and 0.01 for AS and 0.85 and 0.01 for AI. Predicted y-intercepts were 5.4 for pure AS and 10.2 for pure AI. Stable carbon showed no significant correlation with low R^2 and high p-values, indicating non-significance (refer to Table 4).

3.3. Eastern Subtropical Atlantic (ESA)

Bulk POC $\delta^{13}C$ ranged from −20.2‰ to −21.3‰, while $\Delta^{14}C$ ranged from 20‰ to 38‰ (Table 2). TOC (1.3% to 1.7%) and TN (0.2%) values were also lower in ESA than other sites, and C/N_{at} ratios were somewhat higher (9.1 to 10.1). AI isotopic values at

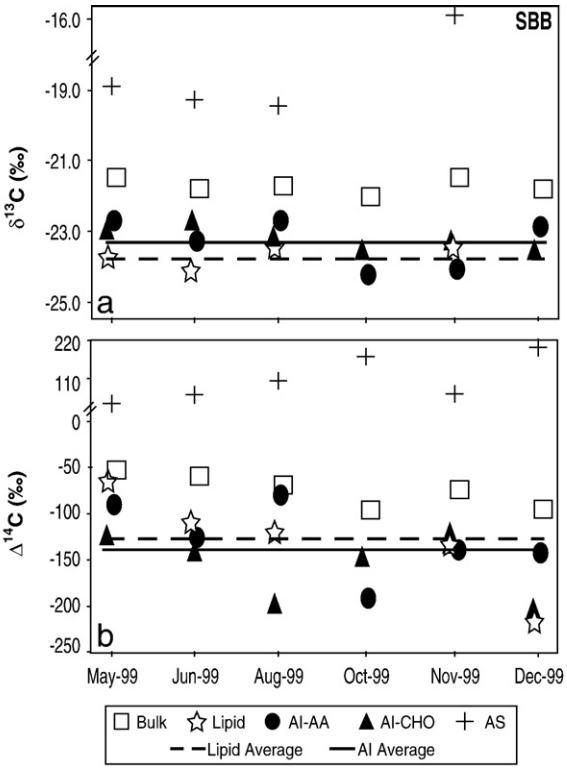

Fig. 2. $\delta^{13}C$ and $\Delta^{14}C$ signatures for POC fractions in the Santa Barbara Basin. Carbon isotopic composition for bulk POC and isolated organic fractions in SBB, May – December 1999. Symbols: Bulk POC=open squares; extractable lipid=open star; AI-AA=solid circle; AI-CHO=solid triangle; AS=cross. Average isotopic values are also indicated by lines: extractable lipids=dotted line; combined AI=solid line. a: $\delta^{13}C$ values for sinking particles collected at 450 m in SBB. b: $\Delta^{14}C$ values for sinking particles collected at 450 m in SBB. Lipid value for Oct-99 not shown because of possible contamination (−379‰). Selective duplicate analyses (Table 3) indicate data uncertainty within range of symbol size.

ESA were generally similar to bulk material. The AI-AA $\delta^{13}C$ ranged from −21.3‰ to −22.1‰, while the AI-CHO fraction ranged from −21.4‰ to −21.9‰, both falling close to $\delta^{13}C$ of bulk POC (Table 3; Fig. 3a). $\Delta^{14}C$ of all AI fractions were modern, with AI-AA values ranging from −2‰ to 15‰ and AI-CHO from −11‰ to 13‰ (Fig. 3b). $\delta^{13}C$ and $\Delta^{14}C$ values between the two AI fractions were highly consistent between samples, with standard deviations for $\delta^{13}C$ values of ±0.1‰ and $\Delta^{14}C$ values of ±2‰. Extractable lipids had substantially lower $\delta^{13}C$ values relative to all other fractions, ranging from −23.9‰ to −24.2‰. $\Delta^{14}C$ values of extractable lipids were also much lower than either bulk OC or the AI fractions, ranging from −55‰ to −91‰. Stable isotopes for calculated AS values ranged from −18.6‰ to −20.0‰ and radiocarbon AS values ranged from 73‰ to 82‰. Overall, low variability observed in all measured values suggests similar annual carbon sources at ESA, and are also consistent with the generally low range in annual primary production (~factor of 3; Wefer and Fisher, 1993), compared to high variation in production at more coastal sites (e.g., ~factor of 10 at SBB; Thunell, 1998). Despite the fact that this is a smaller data set than the others, the uniformity is consistent with what might be expected in oceanic conditions.

Regressions for the ESA site only had three points for each variable, resulting in high *p*-values (indicating lower probability of significance); therefore regression statistics for this location may not be representative of a larger population. $\Delta^{14}C$ of ESA POC had the most significant correlations, *x*=(%AI+Lipid) had R^2 and *p*-values of 0.93 and 0.20, respectively, while *x*=%(AS+lipid) had R^2 and *p*-values of 0.96 and 0.12. The *y*-intercepts were 117‰ for pure AS and −36‰ for pure AI. We note that while *y*-intercepts for other variables were environmentally consistent, less significant correlations were obtained due to a small sample set; coefficients and *y*-intercepts can be found in Table 4.

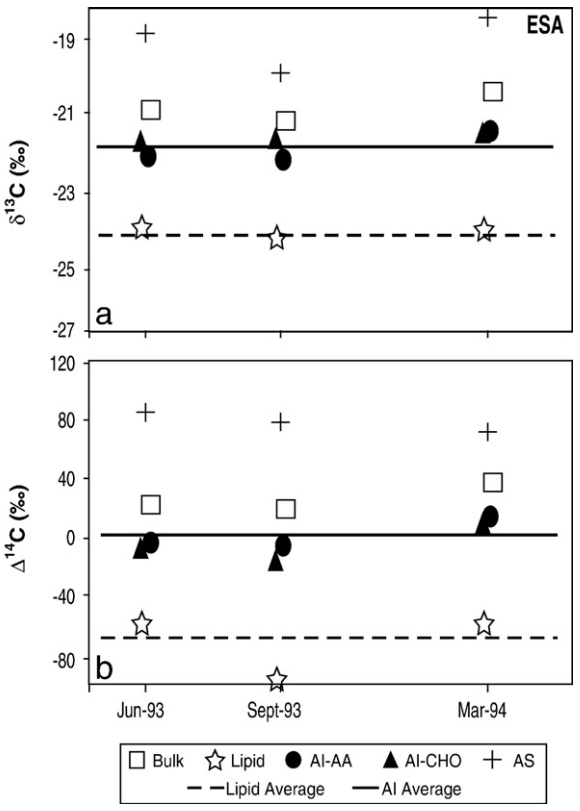

Fig. 3. $\delta^{13}C$ and $\Delta^{14}C$ signatures for POC fractions in the Eastern Subtropical Atlantic. Carbon isotopic composition for bulk POC and isolated organic fractions in ESA, June 1993–March 1994. a: $\delta^{13}C$ values at 3300 m in ESA. b: $\Delta^{14}C$ values at 3300 m in ESA. Selective duplicate analyses (Table 3) indicate data uncertainty within range of symbol size.

3.4. Cariaco Basin (CAR)

Bulk POC $\delta^{13}C$ values were relatively uniform throughout the CAR sample set, ranging from −19.2‰ to −21.8‰ in the shallow trap and −19.0‰ to −22.2‰ in the deep traps (Table 2; Fig. 4a,c), similar to values found in the SBB. A single sample (Feb-99) had substantially higher values in both surface and deep traps (−18.9‰ and −19.2‰, respectively). High values have occasionally been observed in previous studies, attributed to secondary upwelling events in this location (Woodworth et al., 2004), and since the marked $\delta^{13}C$ enrichment was observed at both depths we believe the values are authentic. Bulk $\Delta^{14}C$ values ranged from −7‰ to 49‰ in the shallow sample and 9‰ to 56‰ in the combined deep sample. The lowest $\Delta^{14}C$ values were obtained for samples collected in the fall (Fig. 4b,d). The CAR site had the highest TOC (4.4% to 14.5%) and TN (0.6% to 2.2%) values in the sample set; however, they also showed the greatest annual variability. C/N_{at} ratios were similar in both shallow and deep traps ranging from 7.0 to 8.6.

Across the entire data set for both surface and deep traps, $\delta^{13}C$ of AI-AA ranged from −20.7‰ to −24.0‰ and AI-CHO ranged from −20.1‰ to −23.3‰ (Table 3; Fig. 4a,c). $\Delta^{14}C$ in the AI-AA fraction ranged from −78‰ to 4‰ and AI-CHO from −60‰ to 37‰ (Fig. 4b,d). Overall, as at other sites, average values from the independent AI isolations across the sample set were similar, with standard deviations of ±0.3‰ for $\delta^{13}C$ and ±15‰ for $\Delta^{14}C$. However, unlike at the other sites, these AI $\Delta^{14}C$ isotopic values did not closely resemble either lipids or bulk material, being substantially depleted relative to both. The lipid fractions had the lowest $\delta^{13}C$ values (−21.8‰ to −25.8‰), however CAR lipids displayed generally modern $\Delta^{14}C$ values, similar to those found in bulk samples (−50‰ to 58‰). AS $\delta^{13}C$ and $\Delta^{14}C$ values were within expected ranges for amino acids and carbohydrates, ranging from −17.5‰ to −21.1‰ and 21‰ to 123‰, respectively.

Regression statistics showed strong correlations in the surface traps for both ^{14}C and C/N_{at}. $\Delta^{14}C$ *y*-intercepts were similar to other sites, implying a 105‰ pure AS and −92‰ pure AI endmember. The C/N_{at} *y*-intercepts for pure AS were 6.1, whereas AI had a less nitrogen-rich value of 9.9. The $\delta^{13}C$ regressions had very low R^2 values and low *p*-values (Table 4). Whereas, the deep traps had only one significant correlation for $\delta^{13}C$ vs. %(AS+Lipid), with R^2 and *p*-values of 0.96 and 0.00. The ^{13}C *y*-intercept at this depth was very depleted at −36.3‰.

4. Discussion

The main goals of this study are to examine the origin of the refractory AI material in sinking POC across a range of oceanic environments. We specifically focus on the recent hypothesis that sinking POM material is dominated by lipid-like material (Hwang and Druffel, 2003). Because lipids have distinct (typically lower) stable carbon isotope signatures relative to either bulk biomass or other biochemical classes (e.g., Hayes, 2001), examining $\delta^{13}C$ values of AI together with extracted lipid provides a direct means for evaluating the likely biosynthetic similarity between the two. In contrast, $\Delta^{14}C$ values of AI material does not directly indicate its biochemical composition, but instead provides an

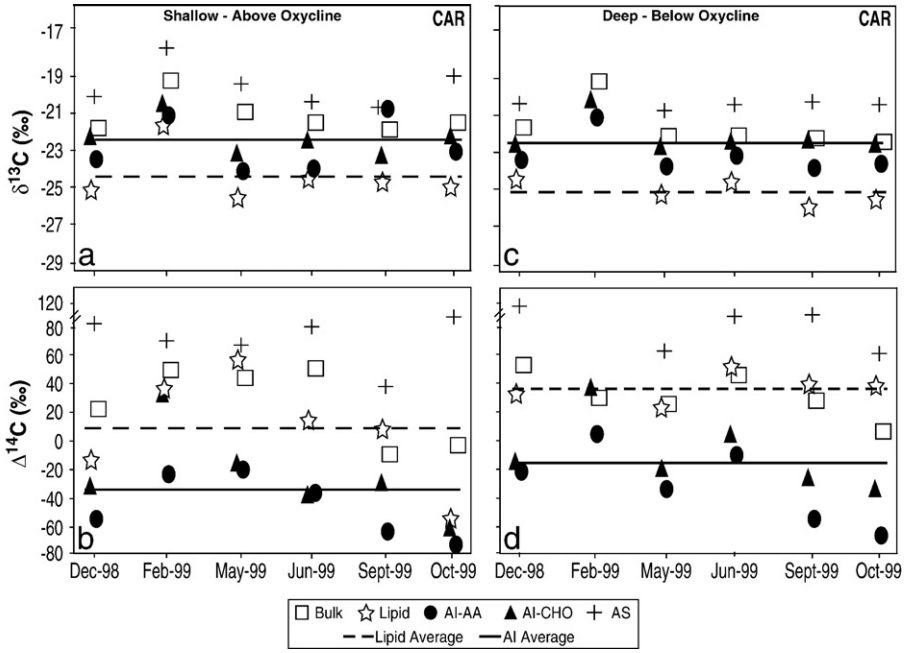

Fig. 4. $\delta^{13}C$ and $\Delta^{14}C$ signatures for POC fractions in the Cariaco Basin. Carbon isotopic composition for bulk POC and isolated organic fractions in CAR, December 1998–October 1999. a, b: $\delta^{13}C$ and $\Delta^{14}C$ values at 275 m (oxic). c, d: $\delta^{13}C$ and $\Delta^{14}C$ values at combined 930 m + 1255 m depths (anoxic). Selected duplicate analyses (Table 3) indicate data uncertainty within range of symbol size.

independent means to evaluate contributions by allochthonous or externally delivered (non-surface), pre-aged carbon sources. Since $\Delta^{14}C$ values are corrected for mass-dependent fractionation (Stuiver and Polach, 1977), all biochemical classes in sinking POC that originate from recent production should have similar $\Delta^{14}C$ signatures, closely linked to $\Delta^{14}C$ values of surface dissolved inorganic carbon (DIC) in a given location at the time of production. Depletion from these expected values indicates either input from non-surface sources or pre-aged material.

The locations from which we examined sinking POC represent a range of oceanic conditions. SBB is a Pacific coastal basin that is closer to the coast, but the in same ocean region where previous work suggested dominant lipid-composition of sinking AI (Hwang and Druffel, 2003). This provides an opportunity to independently examine these previous conclusions using similar methods. The ESA is the most oceanic site examined. While this site is still relatively close to shore (220 km offshore; see *study sites*), it is nevertheless the most similar to the oceanic regions for which the seemingly contradictory non-selective preservation hypothesis has been suggested by Hedges et al. (2001). Finally, the CAR site is an Atlantic margin site, marked by potential terrigenous inputs and an anoxic water column (Goni et al., 2003; Woodworth et al., 2004).

4.1. AI and AS isolations

Unlike previous studies that reported AI-AA exclusively (Hwang and Druffel, 2003; Wang et al., 1998), we independently isolated AI-CHO and AI-AA. Because both H_2SO_4 and HCl acids will hydrolyze biological polymers (e.g., Panagiotopoulos and Sempere, 2005), a-priori these treatments might be expected to leave behind generally similar hydrolysis-resistant material. However, since the acid conditions used for each hydrolysis are targeted to specific compound classes (AA or CHO), it is also possible that there could be broad differences between AI compositions, particularly to the relative proportions of amino acid vs. carbohydrate present.

At both margin sites (CAR — surface and deep; SBB), the nearly equal average ratios of AI-AA vs. AI-CHO (Table 1; 1.2, 0.8 and 0.9 respectively), suggests that despite variation in individual samples, overall either acid treatment yields similar AI amounts. The relatively low variation in AI recoveries (percent standard deviation 6–14%, except 21% for AI-AA in the CAR surface) further suggests that the offsets in average AI amounts in POC (e.g., average CAR = 40% AI; average SBB = 65% AI) are indicative of real differences in POM character at the different sites. It is interesting to note that variability in AI-AA/AI-CHO ratios also seems to consistent with expected variation in sources of POM in different environments. For example, the extremely consistent ratios in SBB (Table 1 — all near 0.9) imply very uniform sources of hydrolysable vs. non-hydrolysable material, whereas CAR ratios indicate the most variable sources (especially in the surface). These results are highly consistent with the contrast in physical parameters and oceanography of these regions, as described above.

In contrast, our oceanic ESA site data (although based on few samples) was distinct from both margin locations, with the average AI-CHO recovery almost twice that of the average AI-AA recovery (74% vs. 40%). The lower AI estimates using the AA acid treatment in ESA samples suggests that proteinaceous material dominates POM in these oceanic samples. This interpretation is

consistent with previous work suggesting that amino acids can dominate total OC in oceanic POM (Hedges et al., 2001; Wakeham et al., 1997a,b). Our results thus suggest there could be a broad distinction between oceanic vs. margin samples in susceptibility to acid hydrolysis method, although this would clearly require further study for verification.

4.1.1. AS: a proxy for labile OM

Since we were not able to independently measure isotopic values of hydrolyzable compound classes (AA and CHO) directly in this study due to small samples sizes (*see* Section 2.2), we calculated total AS material by mass balance as a proxy for these most labile compound classes. AS calculated in a similar manner has previously been shown to be an effective proxy for these compound classes in suspended POM (Hwang et al., 2006b). If this is correct, AS values should have similar $\Delta^{14}C$ signatures to surface DIC values, as well as both freshly produced AA and CHO material. Together, $\delta^{13}C$ and $\Delta^{14}C$ values of AS should provide information on both potential biochemical precursors to AI, as well as the isotopic composition of fresh OM in a given environment (Hwang and Druffel, 2006; Hwang et al., 2006a,b).

Because we are mainly interested in average compositional differences between oceanic regions, and specifically in evaluating the overall *similarity* of average AI vs. lipid material from different regions, we have chosen to average the AI-AA and AI-CHO values throughout each data set. The AI_{avg} is used in the mass balance calculation to determine AS abundance and composition. As one test of this approach, these same mass balance equations were used on data reported in Wang and Druffel (2001), NE Pacific and Southern Ocean surface sediment samples, resulting in very similar predictions to the actual measured values (Southern Ocean — $\Delta^{14}C$ values within 4‰, $\delta^{13}C$ Δ values within 0.2‰; NE Pacific — $\Delta^{14}C$ values within 43‰, $\delta^{13}C$ within 0.4‰). In addition, the strong correlations for AS and AI as we have defined them, and compositional characteristics of POM discussed below (Section 4.5), strongly supports the validity of using $AI_{(avg)}$. While we acknowledge that this approach likely obscures some information in specific samples, and in a few instances yields improbable values likely due to individual outliers (e.g., AS errors in SBB), we feel it is most appropriate to answer our main questions.

In the following discussion, we therefore refer to "AI" in general, and do not further distinguish between the isolations used. Finally, it is also important to bear in mind the intrinsic limitations of operational definitions such as AI. AI has been used in recent literature as a proxy for "refractory" organic matter (e.g., Hwang and Druffel, 2003). Natural OM degradation (or preservation) processes are far more complex than chemical liability to laboratory hydrolysis. However, it is clear from the comparisons of AS vs. DIC ^{14}C, combined with regression results for AI discussed below, our data strongly support this linkage at all locations. Therefore, ^{14}C-depleted AI is in fact a good proxy for refractory OM, and ^{14}C-enriched AS a proxy for fresh production.

4.2. Santa Barbara Basin

Comparison of DIC $\Delta^{14}C$ values previously measured from SBB (Pearson et al., 2000) with calculated AS-values is consistent with the hypothesis that AS represents a proxy for fresh, surface-derived material (Fig. 2b). The low AS $\Delta^{14}C$ values in the spring and summer months (May/June) are likely linked to typically strong upwelling in the CA current system during these times, which resulted in ^{14}C-depleted surface water DIC values (Masiello et al., 1998). In contrast, AS from non-upwelling periods had higher AS $\Delta^{14}C$ values (~50‰), consistent with expected non-upwelling surface water DIC values from the SBB (71‰ in 1996; Pearson et al., 2000). AS $\delta^{13}C$ values were higher than bulk POC or other fractions, consistent with the AS fraction being enriched in amino acids, which typically have higher $\delta^{13}C$ values relative to other biochemical classes (Fig. 2a; Degens et al., 1968; Hayes et al., 1990). This would also be consistent with observations that hydrolyzable amino acids are often the major fraction of hydrolyzable compound classes in fresh plankton and sinking POM, typically a much larger percentage than hydrolyzable sugars (e.g., Hedges et al., 2001; Wakeham et al., 1997b).

In contrast to AS values, ^{14}C values for bulk POC, AI and lipid fractions were all substantially depleted. This offset relative to AS and surface DIC indicates a significant admixture of ^{14}C-depleted material, not directly sourced from surface production, in all these fractions. The generally close correspondence between AI and extractable lipid values for both $\Delta^{14}C$ and $\delta^{13}C$ supports earlier isotopic and spectroscopic analyses indicating that lipid material makes up the majority of refractory carbon in sinking POC in this region (Fig. 2a,b; Hwang and Druffel, 2003; Hwang et al., 2006b). However, these lower values also suggest that the major source of refractory carbon is not selective preservation of material directly exported from the surface, but instead is input from pre-aged carbon reservoirs.

There are a wide variety of possible sources for ^{14}C-depleted carbon in these samples. These include local sources such as resuspended marine sediment (Hwang and Druffel, 2003), OM from eroded bedrock and sedimentary rocks introduced by rivers (Komada et al., 2004), water column sources such as incorporation of "old" marine dissolved organic carbon (DOC) (Druffel et al., 1998; Hwang et al., 2006a), and black carbon from a variety of sources (Dickens et al., 2004; Druffel, 2004; Masiello and Druffel, 1998). The marine $\delta^{13}C$ values and isotopic resemblance to lipids, coupled with the fact that AI material composes 50% or more of sinking POC, suggest a lipid-rich and ultimately marine source. Aged terrigenous carbon is also likely introduced to sediments in this region by episodic riverine input during winter storm events (Thunell, 1998); however the $\delta^{13}C$ values of AI and lipid fractions do not suggest a dominant terrestrial component. $\delta^{13}C$ of bulk POC from CA rivers has been reported to average −24‰ to −25‰ (Peters et al., 1978) and the lipid fraction would thus be expected to be even more depleted (Hayes, 2001). The incorporation of older DOC could also introduce pre-aged carbon with a marine $\delta^{13}C$ signature. However, only a very small fraction of deep-ocean DOC is composed of extractable lipid (Loh et al., 2004; Wakeham et al., 2003). In addition, a relatively small fraction (<15%) of sinking POC has been inferred to derive from the DOC incorporation pathway (Druffel et al., 1998; Druffel and Williams, 1990; Hwang et al., 2006a).

Overall, the most likely source of pre-aged AI carbon at SBB seems the resuspension of marine sedimentary material.

A close correspondence between sediment vs. AI material in sinking POC from another site on the CA margin has recently been demonstrated using solid-state NMR and pyrolysis data (Hwang et al., 2006b), which strongly supports this idea.

4.3. Eastern Subtropical Atlantic

The ESA samples are the deepest sediment trap collection (~3317 m), and also the furthest location from the coast. These samples represent sinking POC that has survived transit through a fully oxic water column, such that only ~1% of original exported OC is expected to remain, dominated by molecularly uncharacterizable material (Hedges et al., 2000; Wakeham et al., 1997b). While not oligotrophic, the much lower productivity, deep water column, and the lack of any direct influence by rivers or seasonal upwelling at this site should make these samples the closest to oceanic sinking POC among the stations examined here.

As in SBB, AS isotopic values are again consistent with protein-rich, directly exported, surface production. The higher AS $\delta^{13}C$ values relative to bulk material (~2‰ enriched), suggests a major component of hydrolyzable amino acid, as expected for oceanic POC (Wakeham et al., 1997b). To the best of our knowledge, DIC $\Delta^{14}C$ have not been measured in this location, but based on other North Atlantic values close to this time period (Druffel, 2002) it is reasonable to assume DIC values ranging from 90–100‰. Our AS $\Delta^{14}C$ values (~100‰) correspond very well with this range, and thus with expected $\Delta^{14}C$ from fresh surface production at the time of sample collection. The $\Delta^{14}C$ values of bulk POC, while modern, are uniformly depleted relative to the AS, suggesting a significant source of pre-aged carbon must again be present in ESA-POC. In contrast to SBB, however, the AI material at ESA does not resemble lipid-like material in either its stable or radiocarbon signatures. The extractable lipids from ESA are depleted in ^{13}C relative to both bulk POC and AI, and have lower $\Delta^{14}C$ values (−70‰ to −90‰) relative to all other fractions (Fig. 3b). Instead, ESA-AI most closely resembles bulk POC isotopic values.

Together, these observations suggest that depleted POC and AI fractions are composed partially from older, non-surface carbon, however that the AI composition is not lipid-like as in SBB. Re-suspended organic carbon (SOC) remains one possible source for this material. While the ESA site is two hundred kilometers from the shelf break, there is evidence that resuspended SOC can be incorporated into sinking POC at similar distances from continental margins (Sherrell et al., 1998), with differences arising from shelf width, sediment load, and ocean energy dynamics (Bauer and Druffel, 1998). However, comparison between AI and extractable lipid values also suggests that if SOC is the source of ^{14}C-depleted material, its composition is quite different from that on the CA margin. The isotopic similarity to bulk material suggests a more even mixture of biochemicals. This conclusion would be consistent with the spectroscopic observations of Hedges et al. (2001) in oceanic POC samples, indicating non-selective preservation of original ratios of biochemical constituents. If SOC is an important source, it is possible that oxic conditions and long transit times may play a role in less preferential preservation of lipids in SOC(Cowie and Hedges, 1992; Ding and Sun, 2005; Grossi et al., 2003; Hedges and Keil, 1995; Wakeham et al., 1997a).

An alternate possibility is that the incorporation of old DOC (Druffel et al., 1998; Hwang et al., 2006a) plays a larger role here, given the sinking particles longer transit time in this much deeper water column. Limited available data suggests that old DOC is in fact selectively incorporated into POC, with mainly the lipid and AI fractions becoming associated with sinking POC (Hwang et al., 2006a). While quantitatively small, the lipid fraction of DOC is also far more ^{14}C-depleted than AI and other fractions (Loh et al., 2004). Incorporation of old DOC would thus be consistent with the offset we observe between AI and lipid ^{14}C ages in the ESA samples.

4.4. Cariaco Basin

CAR is the most complex of these sampling sites, due to bi-seasonal variation in upwelling, terrestrial inputs from rivers, and a fully anoxic water column in the basin below 300 m (Goni et al., 2003; Thunell et al., 2000). The CAR sample set thus provides another view of AI in an ocean margin with more diverse sources than SBB, along with the opportunity to potentially observe any major influence of an anoxic water column on AI composition.

Stable carbon isotope values of upper water CAR samples show similar trends to those observed at SBB margin site (Fig. 4a). The AS ^{13}C values are enriched relative to all other fractions, which is consistent with hydrolyzable amino-acid rich material. DIC $\Delta^{14}C$ in this ocean region has been reported at 94‰ in the early 1990s (Druffel et al., 2005), consistent with this studies' AS values. As in both SBB and ESA, the AS fraction is also substantially enriched in ^{14}C, also consistent with carbon derived from freshly produced surface biomass. The bulk POC $\Delta^{14}C$ is substantially lower and $\delta^{13}C$ is marine, indicating a major input of marine ^{14}C-depleted, pre-aged sources. The AI $\delta^{13}C$ values are depleted relative to both bulk POM and AS, and generally fall close to $\delta^{13}C$ values of the extractable lipid fraction. Thus, as with SBB margin site, CAR data are consistent with the AI fraction having a major component of non-extractable lipids. However, CAR trends in $\Delta^{14}C$ values depart from the SBB pattern in one major respect: instead of falling close to lipid values, $\Delta^{14}C$ of AI in CAR are substantially *depleted* relative to all other fractions (Fig. 4b).

Together with the $\delta^{13}C$ values, these observations suggest that at least CAR-surface AI fractions are dominated by resuspended SOC and, as at SBB, lipids constitute a main component. In contrast to other sites, however, CAR extractable lipids are mostly substantially enriched in ^{14}C relative to AI, with values falling relatively close to bulk material in most samples. This indicates that extractable lipids in CAR have at least some lipid component that is much "younger" (^{14}C enriched) vs. preserved AI material. The contrast with SBB and other sites on the CA margin (Hwang and Druffel, 2003) would suggest that at CAR a much larger relative proportion of newly produced lipids are present in sinking POM. If extractable lipids have major sources from both surface production and resuspended SOC, then such intermediate values would be expected. Extractable lipids are one of the compound classes lost most rapidly with depth in sinking POM degradation (Wakeham et al., 1997a), thus contribution of surface-derived lipids would be expected to be highest in surface POC and then decrease with depth. CAR is the only site in which we had an upper water trap collection, where one would a-priori expect a

greater proportion of surface-derived lipids to be present. For CAR deep samples, it is possible that the anoxic water column has played an important role in preserving lipids with depth (Wakeham et al., 1997a,b), and as discussed below it is also possible that additional chemosynthetic sources of OM could be present (Taylor et al., 2001; Lin et al., 2006).

4.5. Synthesis of AS vs. AI sources and composition

Plotting $\delta^{13}C$ vs. $\Delta^{14}C$ highlights both similarities and differences across our sample suite (Fig. 5). At all sites AS values are most consistent with amino acid-rich, fresh plankton material, while bulk POC, extractable lipid, and AI fractions all show varying degrees of both ^{13}C and ^{14}C-depletion, indicating input from pre-aged marine carbon sources. In general, these values lie on a continuum between enriched AS values (near expected DIC values), through total POC and toward AI, with depleted values in both carbon isotopes (Fig. 5). However positioning of AI relative to other fractions, and in particular the lipid fraction, differs substantially in different regions. This suggests that the nature and dominant sources of refractory material differs broadly between ocean environments. Data from the SBB and CAR surface samples are generally consistent with the conclusions of Hwang and co-authors (Hwang and Druffel, 2003; Hwang et al., 2006a,b), in suggesting that non-extractable lipid material makes up a major part of AI. In contrast, the more oceanic ESA site does not indicate lipid material as the main AI component; instead it has $\delta^{13}C$ and $\Delta^{14}C$ signatures similar to bulk POC, consistent with implications of previous spectroscopic data from open ocean areas (Hedges et al., 2001). The lipid material in ESA plots away from all fractions, consistent with possible pre-aged water column sources. The CAR deep plot is perhaps the most interesting, in that the lipid material clearly plots remotely from other fractions in both isotopes (Fig. 5), suggesting lipids may have additional non-surface derived sources. Additionally, for some samples (fall and winter) $\Delta^{14}C$ values of extractable lipids are actually *higher*

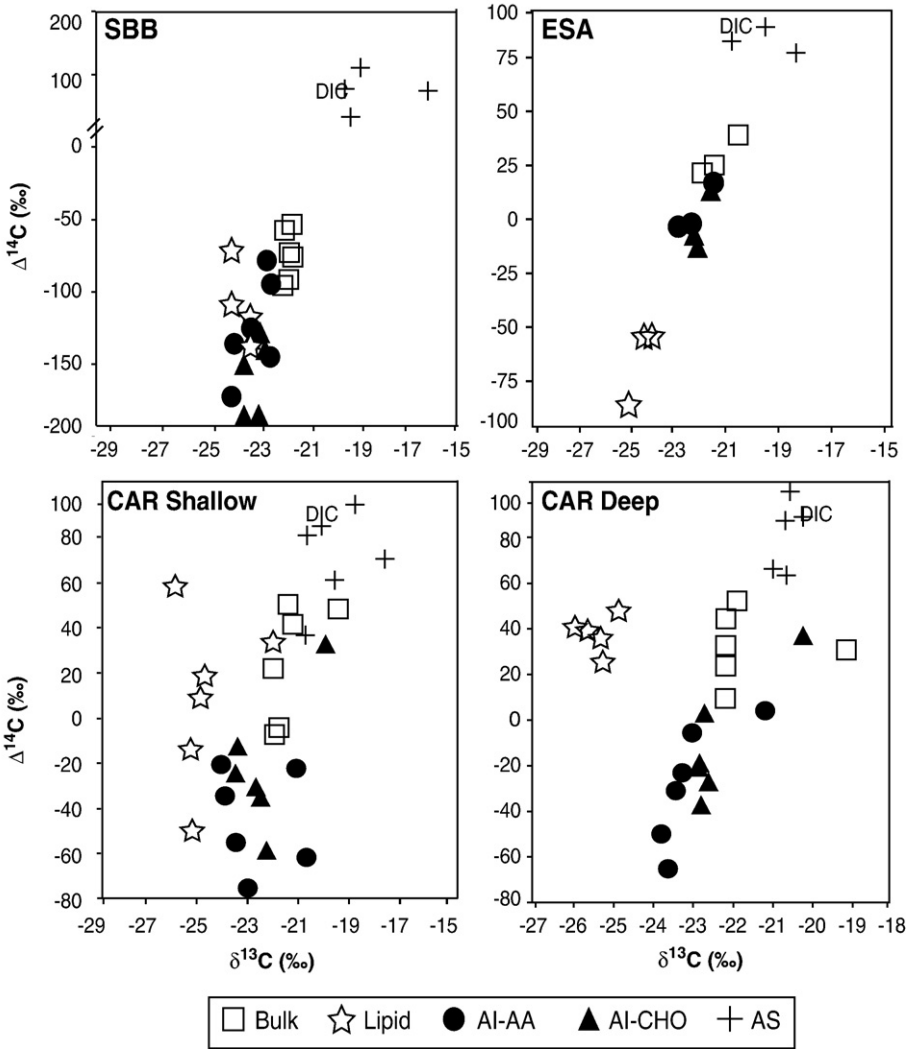

Fig. 5. Comparative $\delta^{13}C$ vs. $\Delta^{14}C$ isotope signatures of all POC fractions. $\delta^{13}C$ (*x*-axis) vs. $\Delta^{14}C$ (*y*-axis) showing relationship of AI fractions relative to bulk POC, lipid, and AS for each sample region. As mentioned in other figures, uncertainty is within range of symbol size. Expected surface DIC values for each region (from previously published data) is indicated by the 'DIC' located on each plot.

than total surface POC $\Delta^{14}C$ values (Fig. 4b). While it is possible that an additional source of surface produced, ^{14}C-enriched lipids may be present in these deep trap samples, another scenario is the addition of freshly synthesized lipid material around the redox transition depth. Such as a chemosynthetic source, which is consistent with the depleted $\delta^{13}C$ values for the lipid cluster vs. other compound classes (Fig. 5), and is supported by results of regression analysis discussed below.

4.5.1. CAR surface, SBB and ESA sample regressions

Regression tests quantitatively test the strength of these relationships, and more clearly define differences in AI and AS across our environments. For sites at which AI and AS are the main carbon sources and have distinct isotopic and elemental compositions, their varying inputs to sinking POC would represent two end-member mixing. Also, the *y*-intercepts of such regressions should indicate the average composition for "pure" AS (or AI) material over the time period sampled. While general slopes of such lines might have similar trends in all ocean regions (i.e., AS is likely always "younger" and AI "older"), specific end-member values would be expected to be linked to specific carbon sources in each location. These values can thus be used to examine our conclusions about AS and AI sources.

Plotting together regressions for %(AI+lipid) vs. $\Delta^{14}C$, C/N_{at} and $\delta^{13}C$ gives simultaneous view of the strength of relationships for each region, showing similarities (or lack thereof) in predicted AS and AI end-members (Fig. 6). Note that the assignment of the lipid fraction may be an important factor in interpreting these plots, because it is likely present in both AS and AI material. Based on results discussed above, in some locations (SBB) lipids would be expected to generally derive from the AI fraction, while in others (ESA) it is more likely evenly partitioned. The two regression tests summarized for each variable (Table 4 and results) thus compare predictions for either the AI or AS by using x=(%AS+lipid) or x=(%AI+lipid) respectively. The regression results suggest that the SBB, ESA, and CAR surface samples all follow very similar trends, whereas the CAR deep samples behave differently, possibly from unique OM sources (Fig. 6a–c). We thus discuss these groupings accordingly.

The strong correlations between AS and both bulk $\Delta^{14}C$ and C/N_{at} values for all these sites strongly supports the idea that overall elemental and isotopic composition can be predicted by two-component mixing between ^{14}C-depleted AI material and AS, where AS is a proxy for freshly exported surface POC (Table 4; Fig. 6a,b). In $CAR_{surface}$ and SBB the *y*-intercepts (indicating $\Delta^{14}C$ of pure AS material; +105‰ and +135‰) are in good agreement with expected average values for $\Delta^{14}C$ of surface DIC. The predicted C/N_{at} values for the AS end-members in all cases are very close to classical Redfield values (6.1 and 5.4). This match with expected fresh plankton compositions further validates our choice of using the 'average' AI recoveries for calculation for the AS proxy. The complementary regressions predicting pure AI (listed in Table 4), indicate substantially depleted ^{14}C values (−92‰ and −169‰), coupled with elevated C/N_{at} ratios (9.9 and 10.2), which further support a sedimentary source for this material. For SBB in particular, the *y*-intercept for AI–$\Delta^{14}C$ aligns very closely with the measured average lipid from this location ($\Delta^{14}C$ of −169‰ and −170‰, respectively), consistent with the hypothesis for sedimentary-lipid dominated material. For ESA the weaker regression *p*-values are due to the small sample size, however the intercepts indicating pure AS ($\Delta^{14}C$ of +117‰; C/N_{at} of 4.8) and AI ($\Delta^{14}C$ of −36‰; C/N_{at} of 13.1) are nevertheless all consistent with our source interpretations. In contrast, practically non-existent correlations are observed for $\delta^{13}C$ at all these sites (Fig. 6c, Table 4), which indicates no systematic offset exists between $\delta^{13}C$ of AI and $\delta^{13}C$ of average AS. This further supports the hypothesis that AI material is ultimately marine-derived in all these regions.

4.5.2. CAR deep sample regressions

For the CAR deep samples, the lack of correlation observed with either $\Delta^{14}C$ or C/N_{at} values ($R^2<0.20$, $p>0.38$) indicates a striking contrast in OM sources and cycling compared to the other sites. This suggests that additional sources of organic matter exist here, rendering our two end-member mixing no longer adequate. It is possible that additional AI or AS sources are both present below the oxycline, and the CAR deep $\delta^{13}C$ results are particularly interesting in this regard. As discussed above (Fig. 5), the CAR deep samples have lipid compositions that appear strongly atypical. It is thus perhaps not surprising that unlike for other sites, correlations for $\delta^{13}C$ are strongly

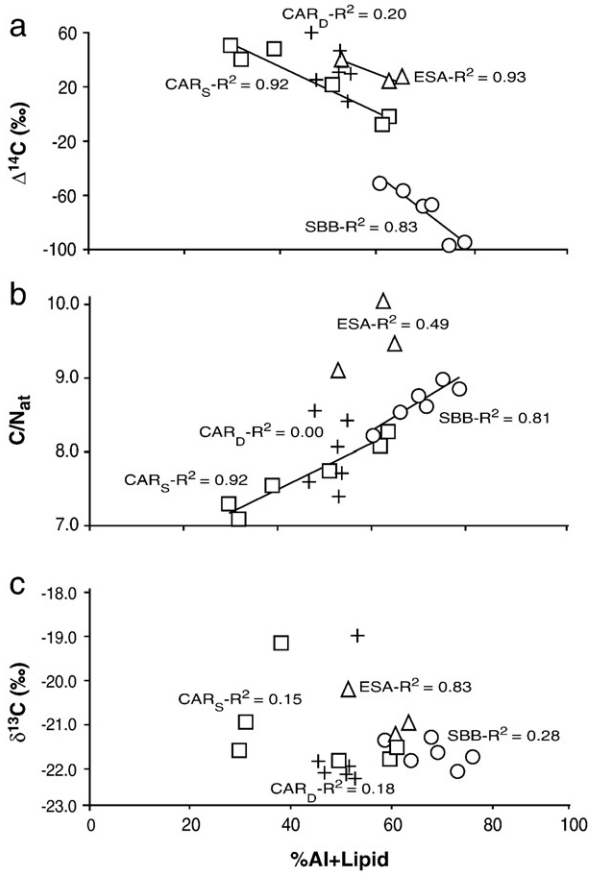

Fig. 6. Regression plots for bulk $\Delta^{14}C$, C/N_{at} and $\delta^{13}C$ vs. %(AI+Lipid). Symbols: SBB=circles; ESA=triangles; CAR surface=squares; CAR deep=crosses; Solid lines are regression trendlines, and are included only for significant regressions (as defined by R^2 and *p*-values in Table 4). Predicted values for pure AS are indicated by *y*-intercept values in Table 4. a: $\Delta^{14}C$ regressions. b: C/N_{at} regressions. c: $\delta^{13}C$ regressions.

affected by assignment of the lipid fraction. The lack of correlation in x=%(AI+Lipid) regressions (Fig. 6c) is similar to other samples. However, unlike at other sites, the complimentary regression (x=%AS+Lipid) shows a strongly significant correlation (Table 4). Once again, this is consistent with the interpretation that an additional source of "fresh" lipids may exist in the deep CAR.

It is of particular interest, that this sites' only significant regression had a highly depleted $\delta^{13}C$ y-intercept value (−36.3‰) projected for pure AI, which aligns well with classical values for chemosynthetic material (Ruby et al., 1987; Taylor et al., 2001). This would suggest that a significant portion of AI material in CAR deep does not originate in surface waters, but is chemosynthetically produced in the water column or in sediments. One should note, however, that this specific intercept is strongly influenced by a single $\delta^{13}C$ value (−19.0‰; see Fig. 6c). Since almost identical depleted values are independently observed in CAR surface for the same time interval (Feb-99), it is likely this is valid data, but it might represent an anomalous period. If the Feb-99 value is removed, a reasonable correlation still remains (R^2=0.68, p=0.06), and the y-intercept (−27.9‰) remains depleted vs. AI in all other sample groups. This latter value for AI end-member seems more reasonable, since surface derived (non-chemosynthetic) POC would still likely compose a substantial portion of sedimentary AI. Alternately, an enhanced contribution of selectively preserved lipid material in CAR deep AI could also contribute to these values.

5. Summary and general hypothesis for AI origin

Our data set strongly suggests that the nature of refractory POC varies broadly between margin and open ocean regions, and that specific non-surface AI sources are key in determining AI amount and composition in a given location. Such differences in AI composition and source, however, do not directly address the pathways of OC alteration or preservation. Previously observed non-selective degradation of sinking POC from several deep water sites (Hedges et al., 2001), combined with seemingly ubiquitous ^{14}C-depleted AI material, suggests a unifying mechanism that can accommodate both sets of observations (Fig. 7).

We hypothesize that non-selective preservation, perhaps facilitated by mineral or other physical protection (Armstrong et al., 2002; Ingalls et al., 2003; Keil et al., 1994; Knicker and Hatcher, 1997), is the major process shaping the composition of the small fraction of sinking primary production which survives original transit through the water column at all locations. The subsequent addition of pre-aged OC from other reservoirs could then explain the variation we observe in AI isotopic signatures. The relative amounts and sources of pre-aged OC would be expected to vary substantially based on oceanic region, with resuspended SOC more prevalent (and its composition more variable) near margins. Importantly, if the main source of pre-aged carbon is marine, as $\delta^{13}C$ values at all our sites indicate, then non-selective preservation during the initial water column transit is only the first (*and ultimately less important*) step in shaping the amount and composition of refractory material actually present in margin POC (Fig. 7a). Degradation in surface sediments, along with associated resuspension and transport, would represent a recycling "loop" through which carbon is not only aged, but its composition altered, apparently selectively concentrating lipid-like AI material in many locations (Aller, 1994; Grossi et al., 2003; Harvey and Macko, 1997; Wakeham et al., 1997a). Terrestrial input is of course also likely to be a component of SOC, and thus important in shaping AI composition in some locations (Komada et al., 2004; Peters et al., 1978).

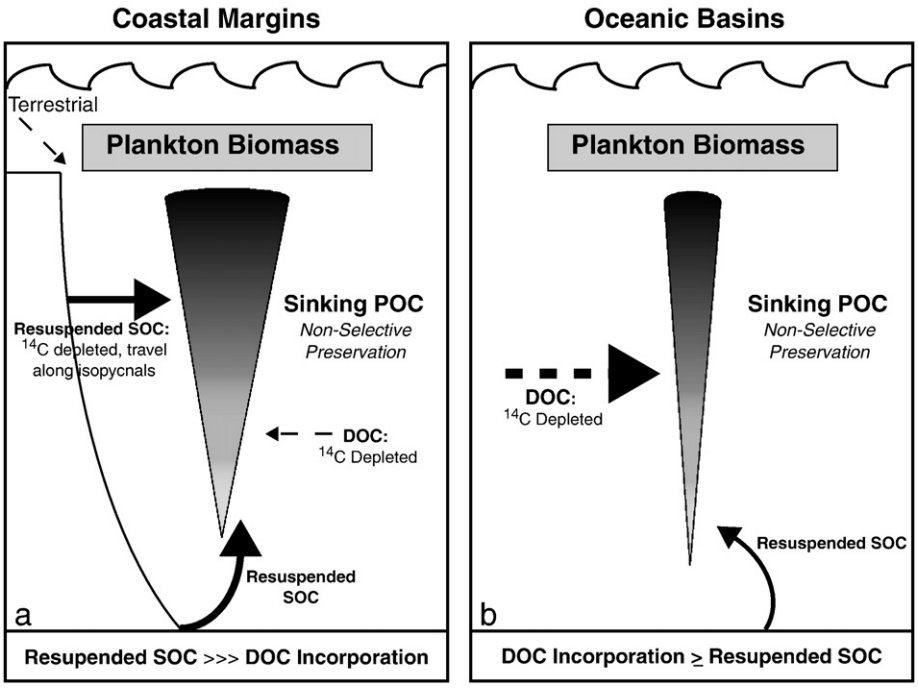

Fig. 7. Conceptual Model of AI composition and sources in POC from margin vs. oceanic environments. Cartoon illustrating a unifying hypothesis regarding major pre-aged ^{14}C sources to sinking POC in margin (a) vs. oceanic (b) regions.

In oceanic regions, while resuspended SOC is also likely present (e.g., Bauer and Druffel, 1998; Druffel et al., 1998), contribution from the adsorption of old DOC components would likely have an additional, and possibly greater, impact (Fig. 7b). A ^{14}C-depleted DOC source (Loh et al., 2004) should be clearly visible in ^{14}C values (specifically of the lipid class; Hwang et al., 2006b), while the overall biochemical composition — as reflected in NMR or the $\delta^{13}C$ values of AI, could remain relatively unchanged. While a hypothesis to be tested, this synthesis would effectively reconcile previous apparently contradictory observations of Hedges et al. (2001) and Hwang and Druffel (2003).

Future work aimed at understanding the composition and preservation mechanisms of sinking particles throughout the ocean should examine additional open ocean sites to minimize influence of resuspended sediments and terrestrial input. One of the most promising approaches for future POC composition research may be in combination of spectroscopic approaches, in particular solid-state NMR, with isotopes of compound classes (e.g., Hwang et al., 2006b). Simultaneous isotopic analysis of POC and surface sediments from oceanic locations, combined with NMR analyses, would be a valuable and direct test of some of our hypotheses.

Together, our data set reinforces the utility of combining organic separations with coupled ^{13}C and ^{14}C isotopic characterization to understand sources and cycling of uncharacterized material in ocean biogeochemical cycles. The strong regression results for AS and AI composition supports mineral acid hydrolysis as a simple and reasonably effective method to partition POC into two distinctly sourced components: "fresh" AS material (whose main source is recent surface biosynthesis) vs. ^{14}C-depleted AI material (whose primary source is *not* recent surface production, but another pre-aged carbon reservoir). An important implication which builds upon many previous $\Delta^{14}C$ based observations (e.g., Druffel et al., 1998; Hwang and Druffel, 2003; Wang et al., 1996, Hwang et al., 2006b) is that a substantial fraction of organic carbon collected by sediment traps, in particular those near continental margins, in fact does *not* represent directly exported surface production, but is "recycled" from other carbon reservoirs. Understanding the varying degree of input in different trap locations may be important in reconciling trap-derived OC fluxes with exported surface productivity. Coupling $\Delta^{14}C$ measurements with AS/AI isolation with direct comparisons to surface DIC values offers a straightforward tool to explore these ratios in different ocean regions.

Acknowledgements

We would like to thank Bob Thunell and Eric Tappa for access to the CAR and SBB sediment trap archives; Leslie Sautter graciously provided sediment trap splits for the ESA site. Deepest thanks to Ian Voparil, Brett Walker, Jenny Lehman, and Paula Zermeno for lab assistance and support. Also, we would like to thank Ellen Druffel for very helpful comments on an early version of the manuscript, Greg Rau and Miguel Goni for invaluable suggestions regarding data treatment, and insightful comments by four anonymous reviewers. Funding was provided by the UC/LLNL Laboratory Directed Research and Development Program (04-ERD-060) and the UCOP Campus Laboratory Collaboration Program. Radiocarbon analyses were performed under the auspices of the U.S. Department of Energy by the University of California's Lawrence Livermore National Laboratory (contract W-7405-Eng-48).

References

Aller, R.C., 1994. Bioturbation and remineralization of sedimentary organic-matter — Effects of redox oscillation. Chemical Geology 114 (3–4), 331–345.
Altabet, M.A., 2001. Nitrogen isotopic evidence for micronutrient control of fractional NO_3 utilization in the equatorial Pacific. Limnology and oceanography 46 (2), 368–380.
Armstrong, R.A., Lee, C., Hedges, J.I., Honjo, S., Wakeham, S.G., 2002. A new, mechanistic model for organic carbon fluxes in the ocean based on the quantitative association of POC with ballast minerals. Deep-Sea Research II 49, 219–236.
Astor, Y., Muller-Karger, F., Scranton, M.I., 2003. Seasonal and interannual variation in the hydrography of the Cariaco Basin: implications for basin ventilation. Continental Shelf Research 23 (1), 125–144.
Bauer, J.E., Druffel, E.R.M., 1998. Ocean margins as a significant source of organic matter to the deep ocean. Nature 392, 482–485.
Bohonak, A.J., van der Linde, K., 2004. RMA: Software for Reduced Major Axis regression, Java version. Website: http://www.kimvdlinde.com/professional/rma.html.
Brown, T.A., Southon, J.R., 1997. Corrections for contamination background in AMS ^{14}C measurements. Nuclear Instruments and Methods in Physics Research B 123, 208.
Cowie, G.L., Hedges, J.I., 1984. Carbohydrate sources in coastal marine-environment. Geochimica et Cosmochimica Acta 48 (10), 2075–2087.
Cowie, G.L., Hedges, J.I., 1992. The role of anoxia in organic-matter preservation in coastal sediments — relative stabilities of the major biochemicals under oxic and anoxic depositional conditions. Org. Geochem. 19 (1–3), 229–234.
Degens, E.T., Behrend, M., Gotthari, B., Reppmann, E., 1968. Metabolic fractionation of carbon isotopes in marine plankton, II. Data on samples collected off the coasts of Peru and Ecuador. Deep-Sea Research I 15, 11–20.
deLeeuw, J.W., Largeau, C., 1993. A review of macromolecular organic compounds that comprise living organisms and their role in kerogen, coal, and petroleum formation. Organic Geochemistry. Plenum Press. 23–72 pp.
Deuser, W., 1973. Cariaco Trench: oxidation of organic matter and residence time of anoxic water. Nature 242, 601–603.
Dickens, A.F., Gelinas, Y., Masiello, C.A., Wakeham, S.G., Hedges, J.I., 2004. Reburial of fossil organic carbon in marine sediments. Nature 427 (6972), 336–339.
Ding, H., Sun, M.Y., 2005. Biochemical degradation of algal fatty acids in oxic and anoxic sediment–seawater interface systems: effects of structural association and relative roles of aerobic and anaerobic bacteria. Marine Chemistry 93, 1–19.
Druffel, E.R.M., 2004. Comments on the importance of black carbon in the global carbon cycle. Marine Chemistry 92 (1–4), 197–200.
Druffel, E.R.M., Bauer, J.E., Griffin, S., 2005. Input of particulate organic and dissolved inorganic carbon from the Amazon to the Atlantic Ocean. Geochemistry Geophysical Geosystem 6 (3), 1–7.
Druffel, E.R.M., 2002. Radiocarbon in corals: records of the carbon cycle, surface circulation and climate. Oceanography 15 (1), 122–127.
Druffel, E.R.M., Griffin, S., Bauer, J.E., Wolgast, D.M., Wang, X.C., 1998. Distribution of particulate organic carbon and radiocarbon in the water column from the upper slope to the abyssal NE Pacific Ocean. Deep-Sea Research II 45 (4–5), 667–687.
Druffel, E.R.M., Williams, P.M., 1990. Identification of a deep marine source of particulate organic carbon using bomb ^{14}C. Nature 347, 172–174.
Fandino, L.B., Riemann, L., Steward, G.F., Long, R.A., Azam, F., 2001. Variations in bacterial community structure during a dinoflagellate bloom analyzed by DGGE and 16S rDNA sequencing. Aquatic Microbial Ecology 23, 119–130.
Goni, M.A., et al., 2003. Biogenic fluxes in the Cariaco Basin: a combined study of sinking particulates and underlying sediments. Deep-Sea Research I 50, 781–807.
Grossi, V., Caradec, S., Gilbert, F., 2003. Burial and reactivity of sedimentary microalgal lipids in bioturbated Mediterranean coastal sediments. Marine Chemistry 81, 57–69.
Harvey, H.R., Macko, S.A., 1997. Kinetics of phytoplankton decay during simulated sedimentation: changes in lipids under oxic and anoxic conditions. Organic Geochemistry 27 (3–4), 129–140.
Hayes, J.M., 2001. Fractionation of carbon and hydrogen isotopes in biosynthesis processes. Reviews in Mineralogy & Geochemistry 43, 225–277.
Hayes, J.M., Freeman, K.H., Popp, B.N., Hoham, C.H., 1990. Compound-specific isotopic analyses — a novel tool for reconstruction of ancient biogeochemical processes. Organic Geochemistry 16 (4–6), 1115–1128.

Hedges, J.I., et al., 2001. Evidence for non-selective preservation of organic matter in sinking marine particles. Nature 409, 801–804.
Hedges, J.I., et al., 2000. The molecularly-uncharacterized component of nonliving organic matter in natural environments. Organic Geochemistry 31, 945–958.
Hedges, J.I., Keil, R.G., 1995. Sedimentary organic matter preservation: an assessment and speculative synthesis. Marine Chemistry 49, 81–115.
Hedges, J.I., Lee, C., Wakeham, S.G., Hernes, P.J., Peterson, M.L., 1993. Effects of poisons and preservatives on the fluxes and elemental compositions of sediment trap materials. Journal of Marine Research 51, 651–668.
Hill, P.S., 1998. Controls on floc size in the sea. Oceanography 11, 13–18.
Honda, M.C., 1996. Inorganic radiocarbon in time-series sediment trap samples: implication of seasonal variation of ^{14}C in the upper ocean. Radiocarbon 38 (3), 583–595.
Honjo, S., Doherty, K., 1988. Large-aperture time series oceanic sediment traps: design objectives, construction and application. Deep-Sea Research I 35, 133–149.
Hulthe, G., Hulth, S., Hall, P.O.J., 1998. Effect of oxygen on degradation rate of refractory and labile organic matter in continental margin sediments. Geochimica et Cosmochimica Acta 62 (8), 1319–1328.
Hwang, J., Druffel, E.R.M., 2003. Lipid-like material as the source of the uncharacterized organic carbon in the ocean? Science 299, 881–884.
Hwang, J., Druffel, E.R.M., 2005. Blank correction for Delta C-14 measurements in organic compound classes of oceanic particulate matter. Radiocarbon 47 (1), 75–87.
Hwang, J., Druffel, E.R.M., 2006. Carbon isotope ratios of organic compound fractions in oceanic suspended particles. Geophysical Research Letters 33 (23).
Hwang, J., Druffel, E.R.M., Bauer, J.E., 2006a. Incorporation of aged dissolved organic carbon (DOC) by oceanic particulate organic carbon (POC): an experimental approach using natural carbon isotopes. Marine Chemistry 98 (2–4), 315–322.
Hwang, J., Druffel, E.R.M., Eglinton, T.I., Repeta, D.J., 2006b. Source(s) and cycling of the nonhydrolyzable organic fraction of oceanic particles. Geochimica et Cosmochimica Acta 70, 5162–5168.
Ingalls, A.E., Lee, C., Wakeham, S.G., Hedges, J.I., 2003. The role of biominerals in the sinking flux and preservation of amino acids in the Southern Ocean along 170W. Deep-Sea Research II 50, 713–738.
Keil, R.G., Montlucon, D.B., Prahl, F.G., Hedges, J.I., 1994. Sorptive preservation of labile organic-matter in marine-sediments. Nature 370 (6490), 549–552.
Knauer, G.A., Karl, D.M., Martin, J.W., Hunter, C.N., 1984. In situ effects of selected preservatives on total carbon, nitrogen and metals collected in sediment traps. Journal of Marine Research 42, 445–462.
Knicker, H., Hatcher, P.G., 1997. Survival of protein in an organic-rich sediment: possible protection by encapsulation in organic matter. Naturwissenschaften 84 (6), 231–234.
Komada, T., Druffel, E.R.M., Trumbore, S.E., 2004. Oceanic export of relict carbon by small mountainous rivers. Geophysical Research Letters 31 (L07504), 1–4.
Lange, C.B., Weinheimer, A.L., Reid, F.M.H., Thunell, R.C., 1997. Sedimentation patterns of diatoms, radiolarians, and silicoflagellates in Santa Barbara Basin, California. California Cooperative Oceanic Fisheries Investigations Reports 38, 161–170.
Largeau, C., deLeeuw, J.W., 1995. Advances in Microbial Ecology. Plenum Press, NY. 77–117 pp.
Lee, C., Cronin, C., 1982. The vertical flux of particulate organic nitrogen in the sea — decomposition of amino acids in the Peru upwelling area and the equatorial Atlantic. Journal of Marine Research 40 (1), 227–251.
Lee, C., Wakeham, S.G., Arnosti, C., 2005. Particulate organic matter in the sea: the composition conundrum. Ambio 33 (8), 565–575.
Lee, C., Wakeham, S.G., Hedges, J.I., 2000. Composition and flux of particulate amino acids and chloropigments in equatorial Pacific seawater and sediments. Deep-Sea Research I 47 (8), 1535–1568.
Lin, X., et al., 2006. Comparison of vertical distributions of prokaryotic assemblages in the anoxic Cariaco Basin and Black Sea by use of fluorescence in situ hybridization. Applied and Environmental Microbiology 72 (4), 2679–2690.
Loh, A.N., Bauer, J.E., Druffel, E.R.M., 2004. Variable aging and storage of dissolved organic components in the open ocean. Nature 430, 877–880.
Masiello, C.A., Druffel, E.R.M., Bauer, J.E., 1998. Physical controls on dissolved inorganic radiocarbon variability in the California Current. Deep-Sea Research II 45 (4–5), 617:642.
Masiello, C.A., Druffel, E.R.M., 1998. Black carbon in deep-sea sediments. Science 280 (5371), 1911–1913.
Minor, E.C., Wakeham, S.G., Lee, C., 2003. Changes in the molecular-level characteristics of sinking marine particles with water column depth. Geochimica et Cosmochimica Acta 67, 4277–4288.
Nagata, T., Kirchman, D.L., 1997. Roles of submicron particles and colloids in microbial food webs and biogeochemical cycles within marine environments. Advances in Microbial Ecology 15, 81–103.
Nakatsuka, T., Hosokawa, A., Handa, N., Matsumoto, E., Masuzawa, T., 1998. ^{14}C budget of sinking particulate organic matter in Japan Trench: a new approach to estimate the contribution from resuspended particles in deep water column. In: Handa, N., Tanoue, E., Hama (Eds.), Biogeochemistry of Marine Organic Matter. T. Terrapub, Tokyo.
Panagiotopoulos, C., Sempere, R., 2005. Analytical methods for the determination of sugars in marine samples: a historical perspective and future directions. L&O: Methods 3, 419–453.
Pearson, A., Eglinton, T.I., McNichol, A.P., 2000. An organic tracer for surface ocean radiocarbon. Paleoceanography 15 (5), 541–550.
Peters, K.E., Sweeney, R.E., Kaplan, I.R., 1978. Correlation of carbon and nitrogen stable isotope ratios in sedimentary organic matter. Limnology and Oceanography 23 (4), 598–604.
Peterson, L.C., Haug, G.H., 2006. Variability in the mean latitude of the Atlantic Intertropical Convergence Zone as recorded by riverine input of sediments to the Cariaco Basin (Venezuela). Paleoceanography, Paleoclimatology, Paleoecology 234, 97–113.
Pinhassi, J., et al., 2003. Spatial variability in bacterioplankton community composition at the Skagerrak–Kattegat front. Marine Ecology Progress Series 255, 1–13.
Ruby, E.G., Jannasch, H.W., Deuser, W.G., 1987. Fractionation of stable carbon isotopes during chemoautotrophic growth of sulfur-oxidizing bacteria. Applied and Environmental Microbiology 53 (8), 1940–1943.
Sherrell, R.M., Field, M.P., Gao, Y., 1998. Temporal variability of suspended mass and composition in the Northeast Pacific water column: relationships to sinking flux and lateral advection. Deep-Sea Research II 45, 733–761.
Stuiver, M., Polach, H.A., 1977. Reporting of C-14 data — discussion. Radiocarbon 19 (3), 355–363.
Suess, E., 1980. Particulate organic carbon flux in the oceans — surface productivity and oxygen utilization. Nature 288, 260–263.
Taylor, G.T., et al., 2001. Chemoautotrophy in the redox transition zone of the Cariaco Basin: a significant midwater source of organic carbon production. L&O 46 (1), 148–163.
Tegelaar, E.W., deLeeuw, J.W., Derenne, S., Largeau, C., 1989. A reappraisal of kerogen formation. Geochimica et Cosmochimica Acta 53, 3103–3106.
Thunell, R.C., 1998. Particle fluxes in a coastal upwelling zone: sediment trap results from Santa Barbara Basin, California. Deep-Sea Research II 45, 1863–1884.
Thunell, R.C., Tappa, E., Anderson, D.M., 1995. Sediment fluxes and varve formation in Santa Barbara Basin, offshore California. Geology 23 (12), 1083–1086.
Thunell, R.C., et al., 2000. Organic carbon fluxes, degradation, and accumulation in an anoxic basin: sediment trap results from the Cariaco Basin. Limnology and Oceanography 45 (2), 300–308.
Vogel, J.S., Southon, J.R., Nelson, D.E., 1987. Catalyst and binder effects in the use of filamentous graphite for AMS. Nuclear Instruments and Methods in Physics Research B 29 (1–2), 50–56.
Vogel, J.S., Southon, J.R., Nelson, D.E., Brown, T.A., 1984. Performance of catalytically condensed carbon for use in accelerator mass spectrometry. Nuclear Instruments and Methods in Physics Research B 289.
Wakeham, S.G., Hedges, J.I., Lee, C., Peterson, M.L., Hernes, P.J., 1997a. Compositions and transport of lipid biomarkers through the water column and surficial sediments of the equatorial Pacific Ocean. Deep-Sea Research II 44 (9–10), 2131–2162.
Wakeham, S.G., Lee, C., Hedges, J.I., Hernes, P.J., Peterson, M.L., 1997b. Molecular indicators of diagenetic status in marine organic matter. Geochimica et Cosmochimica Acta 61 (24), 5363–5369.
Wakeham, S.G., Pease, T.K., Benner, R., 2003. Hydroxy fatty acids in marine dissolved organic matter as indicators of bacterial membrane material. Organic Geochemistry 34 (6), 857–868.
Wang, X.C., Druffel, E.R.M., 2001. Radiocarbon and stable carbon isotope compositions of organic compound classes in sediments from the NE Pacific and Southern Ocean. Marine Chemistry 73, 65–82.
Wang, X.C., Druffel, E.R.M., Griffin, S., Lee, C., Kashgarian, M., 1998. Radiocarbon studies of organic compound classes in plankton and sediment of the northeastern Pacific Ocean. Geochimica et Cosmochimica Acta 62 (8), 1365–1378.
Wang, X.C., Druffel, E.R.M., Lee, C., 1996. Radiocarbon in organic compound classes in particulate organic matter and sediment in the deep northeast Pacific Ocean. Geophysical Research Letters 23 (24), 3583–3586.
Wefer, G., Fisher, G., 1993. Seasonal patterns of vertical particle flux in equatorial and coastal upwelling areas of the eastern Atlantic. Deep-Sea Research I 40 (8), 1613–1645.
Woodworth, M.P., et al., 2004. Oceanographic controls on the carbon isotopic compositions of sinking particles from the Cariaco Basin. Deep-Sea Research I 51, 1955–1974.